Two-dimensional self-trapped nonlinear photonic lattices

Anton S. Desyatnikov[1], Nina Sagemerten[2], Robert Fischer[1], Bernd Terhalle[2], Denis Träger[2], Dragomir N. Neshev[1], Alexander Dreischuh[1,3], Cornelia Denz[2], Wieslaw Krolikowski[*], and Yuri S. Kivshar[1]

[1]*Nonlinear Physics Center and [*]Laser Physics Center, Center for Ultra-high bandwidth Devices for Optical Systems (CUDOS), Research School of Physical Sciences and Engineering, Australian National University, Canberra ACT 0200, Australia*
[2]*Institute of Applied Physics, Westfälische Wilhelms-Universität Münster, D-48149 Germany*
[3]*Department of Quantum Electronics, Sofia University, BG-1164 Sofia, Bulgaria*
asd124@rsphysse.anu.edu.au

http://www.rsphysse.anu.edu.au/nonlinear

Abstract: We predict theoretically and generate experimentally in photorefractive crystal two-dimensional self-trapped periodic waves of different symmetries, including vortex lattices – patterns of phase dislocations with internal energy flows. We demonstrate that these nonlinear waves exist with nonlocal nonlinearity even when the optically-induced periodic refractive index becomes highly anisotropic, and it depends on the orientation of the two-dimensional lattice relative to the crystallographic c-axis.

OCIS codes: (190.5330) Photorefractive nonlinear optics; (090.7330) Volume holographic gratings; (999.9999) Photonic crystals

References and links

1. Yu. S. Kivshar and G. P. Agrawal, *Optical Solitons: From Fibers to Photonic Crystals* (Academic, San Diego, 2003), 540 pp., and references therein.
2. S. F. Mingaleev, Yu. S. Kivshar, and R. Sammut, in: *Soliton-driven Photonics*, A. D. Boardman and A. P. Sukhorukov, Eds. (Kluwer, Dordrecht, Netherlands, 2001), pp. 487-504.
3. N. K. Efremidis, S. Sears, D. N. Christodoulides, J. W. Fleischer, and M. Segev, "Discrete solitons in photorefractive optically induced photonic lattices," Phys. Rev. E **66**, 046602 (2002).
4. J. W. Fleischer, M. Segev, N. K. Efremidis, and D. N. Christodoulides, "Observation of two-dimensional discrete solitons in optically induced nonlinear photonic lattices," Nature **422**, 147 (2003).
5. D. Neshev, E. Ostrovskaya, Yu. S. Kivshar, and W. Krolikowski, "Spatial solitons in optically induced gratings," Opt. Lett. **28**, 710-712 (2003).
6. A. S. Desyatnikov, E. A. Ostrovskaya, Yu. S. Kivshar, and C. Denz, "Composite band-gap solitons in nonlinear optically induced lattices ," Phys. Rev. Lett. **91**, 153902 (2003).
7. D. Neshev, Yu. S. Kivshar, H. Martin, and Z. G. Chen, "Soliton stripes in two-dimensional nonlinear photonic lattices," Opt. Lett. **29**, 486 (2004).
8. H. Martin, E. D. Eugenieva, Z. Chen, and D. N. Christodoulides, "Discrete solitons and soliton-induced dislocations in partially coherent photonic lattices," Phys. Rev. Lett. **92**, 123902 (2004).
9. S. Minardi, S. Sapone, W. Chinaglia, P. Di Trapani, and A. Berzanskis, "Pixellike parametric generator based on controlled spatial-soliton formation," Opt. Lett. **25**, 326 (2000).
10. Z. Chen, and K. McCarthy, "Spatial soliton pixels from partially incoherent light," Opt. Lett. **27**, 2019 (2002).
11. J. Petter, J. Schröder, D. Träger, and C. Denz, "Optical control of arrays of photorefractive screening solitons," Opt. Lett. **28**, 438 (2003).
12. M. Petrović, D. Träger, A. Strinić, M. Belić, J. Schröder, and C. Denz, "Solitonic lattices in photorefractive crystals," Phys. Rev. E **68**, 055601R (2003).

#10164 - $15.00 USD Received 3 January 2006; revised 12 March 2006; accepted 23 March 2006

13. Ya. V. Kartashov, V. A. Visloukh, and L. Torner, "Two-dimensional cnoidal waves in Kerr-type saturable nonlinear media," Phys. Rev. E **68**, 015603 (2003).
14. A. S. Desyatnikov, D. N. Neshev, Y. S. Kivshar, N. Sagemerten, D. Träger, J. Jägers, C. Denz, and Y. V. Kartashov, "Nonlinear photonic lattices in anisotropic nonlocal self-focusing media," Opt. Lett. **30**, 869 (2005).
15. Z. Chen, H. Martin, E. D. Eugenieva, J. Xu, and A. Bezryadina, "Anisotropic enhancement of discrete diffraction and formation of two-dimensional discrete-soliton trains," Phys. Rev. Lett. **92**, 143902 (2004).
16. A. Sukhorukov, "Soliton dynamics in deformable nonlinear lattices," arXiv:nlin.PS/0507050 (2005).
17. A. S. Desyatnikov, Yu. S. Kivshar, and L. Torner, "Optical vortices and vortex solitons," in *Progress in Optics*, Vol. 47, Ed. E. Wolf (Elsevier, Amstredam, 2005), pp. 219-319.
18. J. Masajada and B. Dubik, "Optical vortex generation by three plane wave interference," Opt. Commun. **198**, 21 (2001).
19. D. Neshev, A. Dreischuh, M. Assa, and S. Dinev, "Motion control of ensembles of ordered optical vortices generated on finite extent background," Opt. Commun. **151**, 413 (1998).
20. A. Dreischuh, S. Chervenkov, D. Neshev, G. G. Paulus, and H. Walther, "Generation of lattice structures of optical vortices," J. Opt. Soc. Am. B **19**, 550-556 (2002).
21. A. Desyatnikov, D. Neshev, and Yu. Kivshar, "Vortex solitons, soliton clusters, and vortex lattices," Ukr. J. Phys. Optics **6**, 71 (2005).
22. D. Jović, D. Arsenović, A. Strinić, M. Belić, and M. Petrović, "Counterpropagating optical vortices in photorefractive crystals," Opt. Express **13**, 4379-4389 (2005), http://www.opticsexpress.org/abstract.cfm?URI=OPEX-13-12-4379.
23. See, e.g., N. R. Cooper, E. H. Rezayi, and S. H. Simon, "Vortex lattices in rotating atomic Bose gases with dipolar interactions," Phys. Rev. Lett. **95**, 200402 (2005), and references therein.
24. A. A. Zozulya, D. Z. Anderson, A. V. Mamaev, and M. Saffman, "Solitary attractors and low-order filamentation in anisotropic self-focusing media," Phys. Rev. A **57**, 522 (1997).
25. G. Bartal, O. Cohen, H. Buljan, J. W. Fleischer, O. Manela, and M. Segev, "Brillouin zone spectroscopy of nonlinear photonic lattices," Phys. Rev. Lett. **94**, 163902 (2005)
26. A. A. Sukhorukov, D. Neshev, W. Krolikowski, and Yu. S. Kivshar, "Nonlinear Bloch-wave interaction and Bragg scattering in optically induced lattices ," Phys. Rev. Lett. **92**, 093901 (2004).
27. A. S. Desyatnikov and Yu. S. Kivshar, "Rotating optical soliton clusters," Phys. Rev. Lett. **88**, 053901 (2002).
28. A. S. Desyatnikov, A. A. Sukhorukov, and Yu. S. Kivshar, "Azimuthons: spatially modulated vortex solitons," Phys. Rev. Lett. **95**, 203904 (2005).
29. D. N. Neshev, T. J. Alexander, E. A. Ostrovskaya, Yu. S. Kivshar, H. Martin, I. Makasyuk, and Z. Chen, "Observation of discrete vortex solitons in optically-induced photonic lattices," Phys. Rev. Lett. **92**, 123903 (2004).
30. J. W. Fleischer, G. Bartal, O. Cohen, O. Manela, M. Segev, J. Hudock, and D. N. Christodoulides, "Observation of vortex-ring discrete solitons in 2D photonic lattices," Phys. Rev. Lett. **92**, 123904 (2004).

1. Introduction

Many novel possibilities to control light propagation, as well as steering and trapping of optical beams, become accessible in nonlinear periodic photonic structures [1]. Periodic modulation of the refractive index changes dramatically the wave band-gap spectrum and diffraction. The interplay between diffraction and periodicity consequently strongly affects the propagation and localization of light, leading to the formation of novel types of self-trapped optical beams, discrete and gap spatial solitons [2].

Photonic lattices can be induced optically in photorefractive crystals employing their anisotropic electro-optic properties [3, 4, 5]. In this approach, an ordinary-polarized periodic light pattern created by several interfering plane waves induces a change of the refractive index via the strong electro-optic effect, while propagating linearly along the crystal. The induced periodic refractive index follows the light intensity distribution and it forms a two-dimensional (2D) photonic lattice, being uniform in the direction of propagation. On the other hand an extraordinary polarized signal beam propagates in the periodically modulated medium and simultaneously is affected by the strong photorefractive screening nonlinearity.

Another important possibility to create stationary two-dimensional light patterns for all-optical induction is offered by the self-trapped periodic waves. Indeed, the diffractionless light patterns in the form of stationary nonlinear periodic waves can propagate without change in their profile, becoming the eigenmodes of the self-induced periodic potentials. This behavior is generic, since nonlinear periodic waves can exist in any type of nonlinear media, not re-

#10164 - $15.00 USD Received 3 January 2006; revised 12 March 2006; accepted 23 March 2006

stricted to photorefractive crystals. Such nonlinear periodic waves can be considered as flexible structures because the lattice is modified and shaped by the nonlinear medium. Such flexible nonlinear photonic lattices offer many novel possibilities for the study of nonlinear effects in periodic systems, because they can interact with localized signal beams via the cross-phase modulation and can form composite bound states [6, 7, 8].

Nonlinear photonic lattices created by two-dimensional arrays of *pixel-like* spatial solitons have been demonstrated experimentally in parametric systems [9], and in photorefractive crystals [10, 11]. For the latter case of two-dimensional arrays of *in-phase* spatial solitons created by the amplitude modulation, every pixel of the lattice induces a waveguide which can be manipulated by an external steering beam [11, 12]. However, the spatial periodicity of these two-dimensional soliton lattices is limited by attractive interaction of the neighboring solitons that generates their strong instability. In contrast, the recently suggested two-dimensional square lattices created by *out-of-phase* spatial solitons were demonstrated to be robust in the isotropic saturable model [13]. The phase profile of such self-trapped waves resembles a chessboard pattern with the lines of π-phase jumps between the neighboring sites.

Recently, we demonstrated experimentally the generation of lattices with the four-fold symmetry in an anisotropic photorefractive crystal [14]. Changing the orientation of the lattice with respect to the c-axis of the photorefractive crystal, we distinguish two types of nonlinear periodic waves: the square pattern, with one high symmetry axis oriented parallel to the c-axis, and diamond pattern, tilted by 45° with respect to the c-axis. Anisotropy of the photorefractive media was shown to affect significantly the diffraction of the propagating waves [15], but even more importantly, it changes the symmetry properties of the induced refractive index pattern because of the combined effect of saturation and nonlocality [14].

In this paper, we perform a generic study on the different symmetry-types of two-dimensional nonlinear periodic waves and reveal their rich variety of symmetries and nontrivial phase structures. We demonstrate, that such periodic waves can be generated in anisotropic photorefractive materials, possessing orientational-dependent structure. First, we study theoretically the phase-modulated two-dimensional structures of *a square geometry*, using *an anisotropic nonlocal model* of photorefractive nonlinearity, in both self-focusing and self-defocusing nonlinear media. We then expand our analysis and introduce novel symmetry-types of two-dimensional nonlinear modes with edge-type phase dislocations and three-fold symmetry, *triangular lattices*. Similar to the two distinct orientations for square lattices, we distinguish the triangular patterns with one of the three dislocation lines oriented parallel or perpendicular to the crystal axis. Again the differences appear in the distribution of the refractive index, and they became more pronounced for larger intensities of the lattice wave, i.e., in the regime of higher saturation. We demonstrate experimentally how this orientational dependence changes the guiding properties of the photonic lattice.

Second, we explore two-dimensional nonlinear lattices with an internal energy flow, which is expected to strongly influence the interaction of the lattice with additional signal beams due to the exchange of momenta between the interacting waves [16]. The net energy flow within the stationary wave structure should be balanced out, thus it will contain closed loops of currents, or optical vortices [17]. *Vortex lattices* were studied in linear [18] and self-defocusing nonlinear optical media [19, 20]. Recently, we predicted the existence of self-trapped vortex lattices of a square symmetry in isotropic saturable nonlinear media [21]. This approach can be generalized to composite lattices created by the counter-propagating waves [22] and it is closely related to the extensively studied vortex lattices in matter waves [23]. In this work, we study the square and hexagonal nonlinear periodic waves with phase dislocations. The square vortex lattice has a four-fold symmetry of the intensity and phase distributions, while the hexagonal intensity pattern is built with the honeycomb structure of vortices.

#10164 - $15.00 USD Received 3 January 2006; revised 12 March 2006; accepted 23 March 2006

The paper is organized as follows. In the next Section, we describe our theoretical model applied to the lattices with the four-fold symmetry, i.e. the square and diamond patterns, including the media with self-focusing and self-defocusing photorefractive nonlinearities. In Section 3 we describe our experimental technique of the phase imprinting and demonstrate a good correspondence between theoretical and experimental results. In Section 4 we expand our analysis to the three-fold symmetry structures and find triangular lattices of two different orientations with respect to the *c*-axis of the crystal. In Section 5 we describe theoretically and experimentally the formation and nonlinear propagation of lattices with nontrivial vortex-like phase patterns.

2. Phase-modulated lattices: theoretical background

Spatially periodic nonlinear modes appear naturally due to a combined action of self-focusing and modulational instability [1]. When the self-focusing effect compensates for diffraction of the optical beams, it may support both isolated spatial solitons and periodic soliton-type lattices. The latter can be identified as *stationary periodic nonlinear waves*, and they include well studied *cnoidal waves*, described by the *cn* and *dn* Jacobi elliptic functions as the stationary solutions of the generalized nonlinear Schrödinger (NLS) equation [1],

$$i\frac{\partial E}{\partial z}+\frac{\partial^2 E}{\partial x^2}+\frac{\partial^2 E}{\partial y^2}+n(I)E=0, \tag{1}$$

where $I\equiv|E|^2$ is the light intensity. Similar nonlinear waves appear as periodic solutions of different nonlinear models, including quadratic, Kerr-type saturable, and photorefractive anisotropic nonlocal models.

In the case of photorefractive, anisotropic and nonlocal model, the nonlinear contribution to the refractive index in Eq. (1) is given by [24]

$$n(I)=\sigma\Gamma\frac{\partial\varphi}{\partial x}, \tag{2}$$

where the parameter $\Gamma=x_0^2\kappa^2 n_0^2 r_{\rm eff}\mathscr{E}$ is defined through the effective electro-optic coefficient $r_{\rm eff}$ and externally applied bias electrostatic field $\mathscr{E}$. The dimensionless parameter $\sigma=\pm1$ indicates the polarity of the applied voltage that changes the character of the photorefractive screening nonlinearity: self-focusing, for $\sigma=+1$, or self-defocusing otherwise. The electrostatic potential φ of the optically-induced space-charge field pattern satisfies the equation:

$$\nabla_\perp^2\varphi+\nabla_\perp\varphi\nabla_\perp\ln(1+I)=\partial_x\ln(1+I), \tag{3}$$

where we use the standard notation $\nabla_\perp$ for the two-dimensional gradient operator such that $\nabla_\perp^2=\partial_x^2+\partial_y^2$, and the intensity I is measured in units of the background (dark) illumination intensity, required for the formation of spatial solitons in this medium. The physical variables $\tilde{x}$, $\tilde{y}$, and $\tilde{z}$ correspond to their dimensionless counterparts as $(\tilde{x},\tilde{y})=x_0(x,y)$ and $\tilde{z}=2\kappa x_0^2 z$, here x_0 is the transverse scale factor and $\kappa=2\pi n_0/\lambda$ is the carrier wave vector with the linear refractive index n_0. Stationary solutions to the system (1)-(3) are sought in the standard form, $E(x,y,z)=U(x,y)\exp(ikz)$, where the field envelope U satisfies the equation

$$-kU+\frac{\partial^2 U}{\partial x^2}+\frac{\partial^2 U}{\partial y^2}+\Gamma U\frac{\partial\varphi}{\partial x}=0. \tag{4}$$

Following Ref. [14], first we look for periodic solutions of a square symmetry, $U(X,Y)=U(X+2\pi,Y+2\pi)$, and solve Eqs. (3), (4) using the relaxation technique [24] with the initial ansatz in the form of a linear periodic mode,

$$U_{\rm lin}(X,Y)=A\ \sin X\ \sin Y. \tag{5}$$

#10164 - $15.00 USD Received 3 January 2006; revised 12 March 2006; accepted 23 March 2006

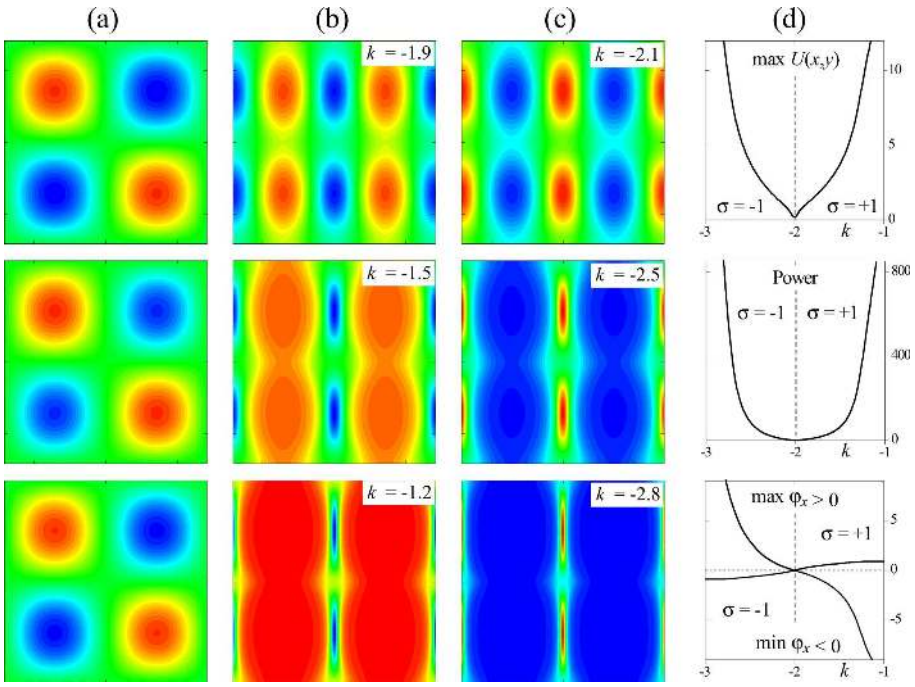

Fig. 1. Comparison between the nonlinear square lattices in self-focusing (b, $\sigma = +1$), and self-defocusing (c, $\sigma = -1$) media. The field $U(x,y)$ in (a) and refractive index $\partial_x \varphi$ in (b,c) are shown for three distinct values of the mode amplitude max $U(x,y)$, or the propagation constant k, from low ($k = -1.9$ and $k = -2.1$) to high ($k = -1.2$ and $k = -2.8$) saturation. Colors are scaled, and the information about the absolute values of the mode amplitude, power density, and the refractive index modulation is summarized in (d).

We find that at least two distinct families of such solutions bifurcate from the linear wave $U_{\rm lin}(X,Y)$, depending on its spatial orientation: *a square lattice* parallel to the c-axis with $X = x$ and $Y = y$, and *a diamond lattice* oriented diagonally, in the latter case $X = (x+y)/\sqrt{2}$ and $Y = (x-y)/\sqrt{2}$. Fig. 1 and Fig. 2 show the field and refractive index for the three values of the lattice intensity, corresponding to the low, moderate, and high saturation regimes for both families of periodic modes, respectively. In a general case $\Gamma \neq 1$, the existence region of these two families occupy a band $k \in [-2, \Gamma - 2]$ with the amplitude $A(k)$ and power density $P(k)$ vanishing in the linear limit $k \to -2$, see Fig. 1(d) and Fig. 2(d). Here the power density is defined as the power of a unit cell, $P = 4 \int \int_0^\pi U^2 dX dY$. The main difference between the solutions with different orientations comes from the structure of the refractive index, as is clearly seen comparing Fig. 1(b) and Fig. 2(b). In the regime of high saturation of nonlinearity the regions with the effective focusing lenses are well separated for the diamond lattice [see Fig. 2(a-d)], and fuse effectively to vertical lines for the square lattice [see Fig. 1(a-d)]; this happens due to larger nonlocality in the limit of strong nonlinearity saturation. In Fig. 1(d) and Fig. 2(d), we plot the maximum and minimum values (extrema) of the refractive index, Extr$(\partial \varphi / \partial x)$.

The model (2) includes the self-defocusing nonlinearity which can be realized with reversing the polarity of the bias external field applied to a photorefractive crystal. In this case $\sigma = -1$ and we also find numerically the stationary periodic square lattices, a two-dimensional analog of the *sn*-type one-dimensional cnoidal waves. The corresponding families of such periodic solutions [Fig. 1(c) and Fig. 2(c)] are compared to the four-fold symmetry lattices in a self-

#10164 - $15.00 USD Received 3 January 2006; revised 12 March 2006; accepted 23 March 2006

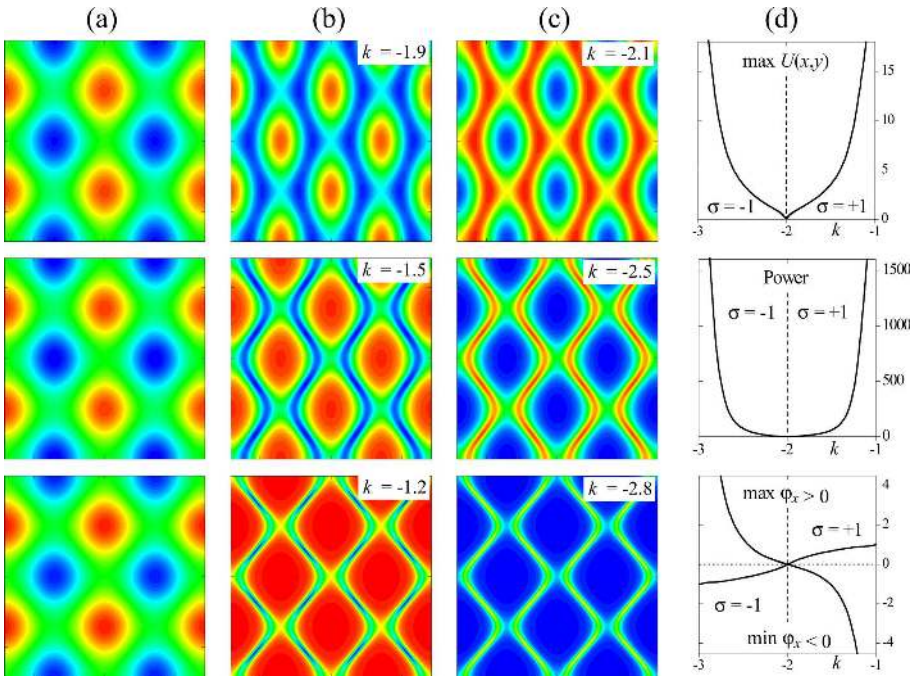

Fig. 2. Same as in Fig. 1 but for the diamond lattices.

focusing medium. We notice that, while the field distribution is almost identical in both cases, the refractive index is opposite: the positive maxima in the self-focusing case (focusing lenses) is inverted for $\sigma = -1$, and it represents defocusing lenses (induced potential maxima). Parameters of two families for $\sigma = \pm 1$ in Fig. 1(d) and Fig. 2(d) are almost symmetric with respect to the linear solution at $k = -2$, however, these two families correspond to different existence domains.

3. Experimental approach

To demonstrate experimentally both the existence and stability of the nonlinear periodic lattices generated in anisotropic and nonlocal photorefractive media, we use an experimental setup similar to that employed earlier [14], shown in Fig. 3. We use a cw frequency-doubled Nd:YAG laser at a wavelength of 532 nm. The laser beam is originally expanded in a beam expander combined with a spatial filter and is subsequently sent through a combination of a quarter wave plate, a programmable spatial light modulator and a polarizer in order to induce the desired phase structure onto the beam. In the inset of Fig. 3 two patterns imprinted onto the modulator are depicted, with bright fields representing zero phase change and dark fields representing phase change of π. The output of the modulator is then imaged by a high numerical aperture telescope onto the front face of our 20 mm long Strontium Barium Niobate (SBN) photorefractive crystal. The polarization of the beam is orientated parallel to the crystalline c-axis, thus the beam will experience a strong photorefractive nonlinearity (the electro-optic coefficient $r_{33} \approx 200$ pm/V). The crystal is biased by an externally applied electric field and uniformly illuminated with a white-light source to control the dark irradiance. Either the front face or the back face of the crystal can be imaged with a lens onto the CCD-camera. The periodic pattern generated by the modulator is filtered in its Fourier plane by an iris diaphragm. The input then

#10164 - $15.00 USD Received 3 January 2006; revised 12 March 2006; accepted 23 March 2006

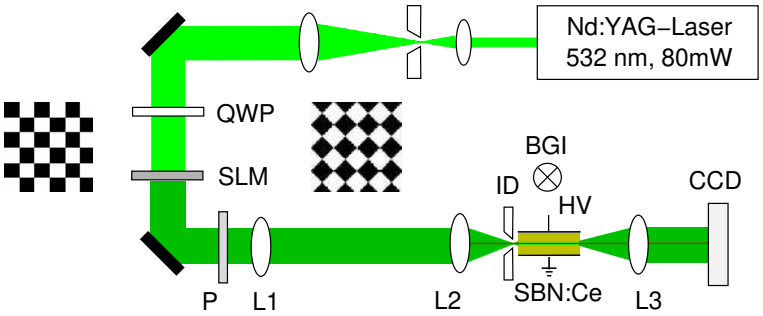

Fig. 3. Experimental setup, QWP – quarter wave plate, SLM – spatial light modulator, P – polarizer, L – lens, ID – iris diaphragm, BGI – background illumination, HV – High voltage, CCD – CCD camera. The insets show the chessboard-like phase patterns for square (left) and diamond (right) lattices, phase values are π (black) and 0 (white).

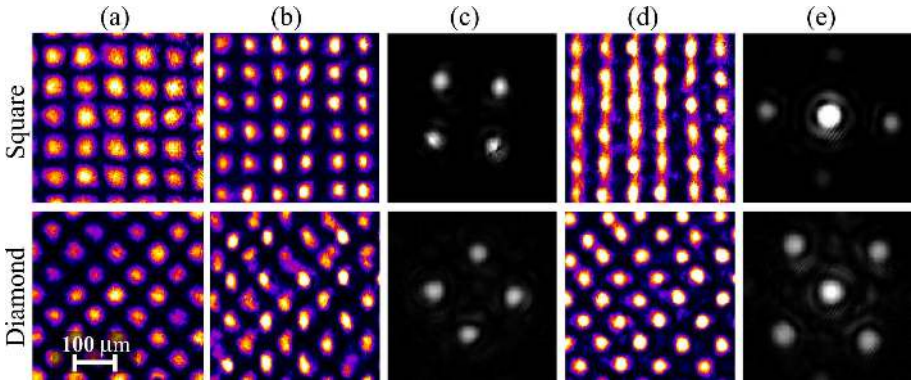

Fig. 4. Experimentally generated light intensity patterns with chessboard-like phase: square (upper row) and diamond (lower row). (a) linear output without applied electric field, (b) nonlinear output with applied electric field, (d) guiding of a plane wave in photonic lattice. (c) and (e) demonstrate the far field structure of the lattice and guided waves in (b) and (d) respectively.

represents a non-diffracting wave, and it experiences robust linear propagation inside the crystal (at zero bias voltage). When bias voltage is applied onto the crystal, the output intensity pattern changes and nonlinear index change is induced in the crystal. In order to probe this refractive index change and establish correspondence to the numerical simulations of the refractive index, the modulator can be switched off so that a broad plane wave illuminates the crystal. Due to the slow response of the photorefractive nonlinearity, we can quickly monitor the output of the plane wave without modifying the induced refractive index change. The plane wave is guided by the periodic array of waveguides induced in the medium and the output intensity pattern of the guided beam qualitatively maps the induced refractive index modulation.

In Fig. 4, we summarize our experimental results for the four-fold symmetry self-trapped lattices: square (top) and diamond (bottom) patterns. Both were measured at a bias field of 1 kV/cm and a total power 1.4 μW. The lattices have the period of 65 μm and their linear output, i.e. output intensity distribution at zero applied voltage, is shown in Fig. 4(a). The intensity distribution for square and diamond patterns is nearly the same and only differs in spatial orientation. When bias voltage is applied on the crystal, the lattice transforms into an eigenmode of its self-induced waveguiding structure and the nonlinear outputs are shown in Fig. 4(b).

#10164 - $15.00 USD Received 3 January 2006; revised 12 March 2006; accepted 23 March 2006

We also monitor the far field (Fourier image) of the lattice wave [see Fig. 4(c)]. In the case of a four-fold lattice symmetry, the far field is represented by four beams, which also determine the boundaries of the first Brillouin zone [25]. The intensity of the plane wave guided by the photonic lattice is shown in Fig. 4(d) and its Fourier image in Fig. 4(e). Accordingly to the theory of the excitation of Bloch waves in periodic structures [26], the plane wave with zero transverse wave-vector corresponds to the central high-symmetry point of the first Brillouin zone [central dominating peak in Fig. 4(e)] and, due to periodicity, it also excites the central points in *higher-order* bands of the transmission spectrum. Thus, the four side beams, visible in Fig. 4(e), indicate the central points of the *second band from the extended Brillouin zone*.

At the same time, the output intensity of the guided wave matches the induced nonlinear refractive index change and can be compared to the profiles of the numerically calculated refractive index in Fig. 1 and Fig. 2. One can clearly see the difference in the refractive indices for two orientations caused by the anisotropy of the photorefractive crystal. Figs. 4(d) demonstrate this difference in the guiding properties of both lattices. Indeed, for square intensity pattern in Fig. 4(d,top), neighboring spots fuse into vertical lines because of nonlocality and do so preferably in one direction because of anisotropy. Corresponding Fourier image demonstrates two dominant side beams generated by the resonant reflections in the guiding structure, corresponding to the one-dimensional periodic pattern oriented vertically. This experimental result supports the numerical predictions, compare with Fig. 1(b) for $k=-1.5$. In contrast, the diamond pattern shows well-pronounced 2D array of waveguiding channels, see Fig. 4(d,bottom) and Fig. 2(b), and its Fourier image contains all four side beams.

4. Triangular lattices

If we expand our theoretical analysis to the studies of the nonlinear stationary structures with the real envelope $U(x,y)$, then the only type of the phase modulations allowed is the edge-type π phase jumps that produce the lines of zero intensity in the lattice. The simplest pattern of this kind with the three-fold symmetry is a triangular lattice. The corresponding linear mode can be constructed by interference of six plane waves, and it can be presented in the following form:

$$U_3(X,Y)=A\sin\left(2Y/\sqrt{3}\right)\sin\left(Y/\sqrt{3}+X\right)\sin\left(Y/\sqrt{3}-X\right), \tag{6}$$

where we assume that one of the dislocation lines is parallel to the X-axis, so that two orientations of this pattern with respect to the crystal c-axis in Eq. (4) will correspond to $(X,Y)=(x,y)$ for the parallel orientation, and, e.g., $(X,Y)=(y,x)$, for the perpendicular orientation. For the linear wave, the value of k is given by $\nabla_\perp^2 U_3/U_3=-16/3\approx=-5.3$. The periodicity of the refractive index pattern is defined by the intensity distribution, not by the field, and in our notation this distance between the closest neighboring peaks of the intensity is $\pi/2$.

We find two distinct families of triangular stationary waves in the self-focusing photorefractive media from low to high saturation regimes, $k>-5.(3)$. We summarize our numerical and experimental data in Fig. 5, where we compare numerical results with experimental images, for both parallel and perpendicular orientations, and for low and high saturations. Experimentally, for switching from low to high saturation, the total power of the lattice-governing beam as well as the intensity of the background illumination are changed. In the nonlinear output, the lattice period is about $48\,\mu$m.

Lattices with parallel orientation display distinct features in their refractive index profile, namely two out-of-phase lobes of the field distribution, which are the closest neighbors in the vertical direction, induce joined humps or focusing "islands". These structures resemble bound dipole pairs studied earlier in Ref. [24]. In the high saturation regime [see Fig. 5(top)], these dipole-islands form a pattern with essentially square symmetry, similar to the diamond pattern

#10164 - $15.00 USD Received 3 January 2006; revised 12 March 2006; accepted 23 March 2006

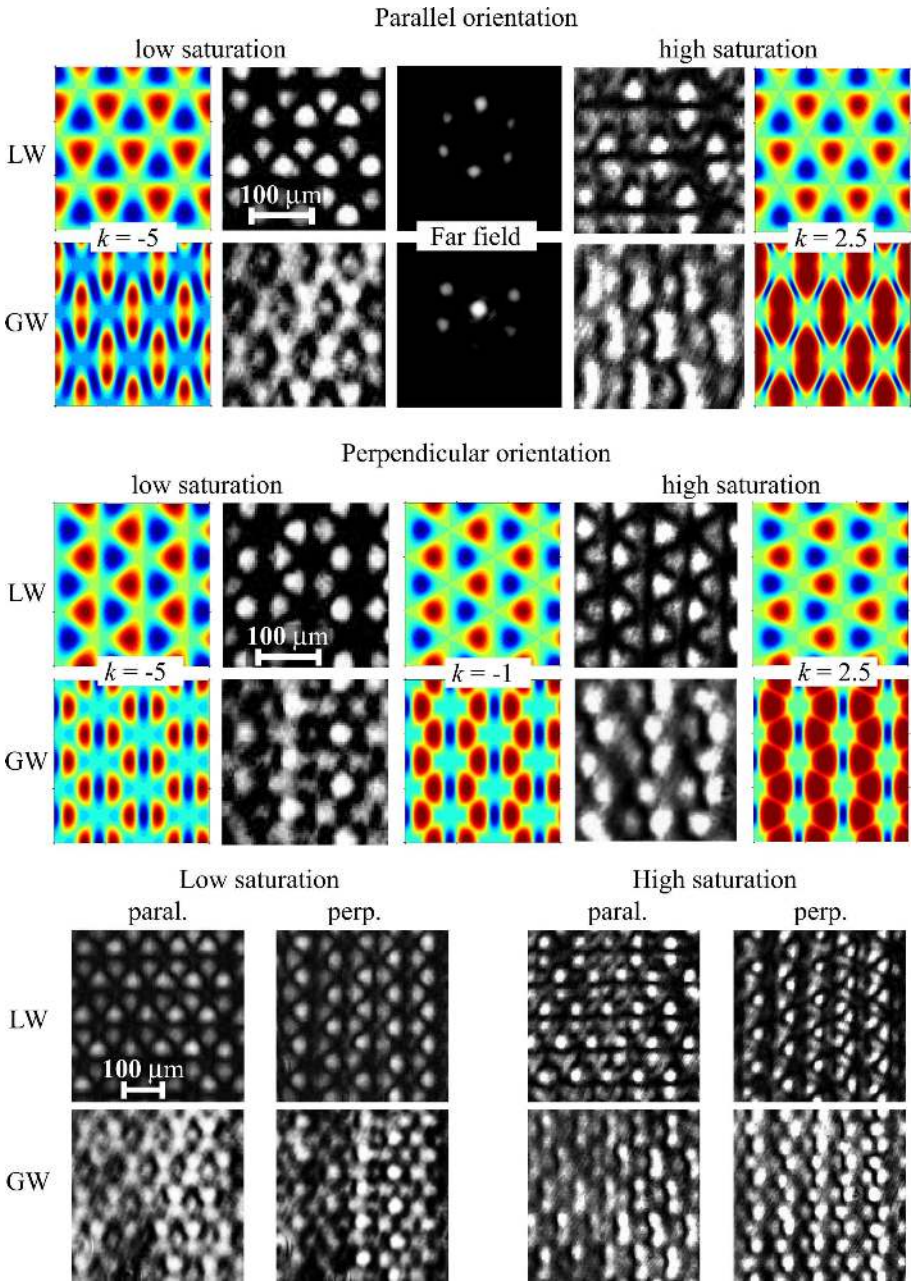

Fig. 5. Theoretical (color) and experimental (grayscale) results for triangular lattices created by interference of six plane waves, see far field images in the top panel. Two distinct orientations of the triangular lattices are compared (top and middle panel) as well as low (left) and high (right) saturation regimes. LW, field $U(x,y)$ (color) and intensity (grayscale) of the lattice wave. GW, calculated profiles of the refractive index (color) and measured intensity of the guided wave (grayscale).

#10164 - $15.00 USD Received 3 January 2006; revised 12 March 2006; accepted 23 March 2006

discussed above. Experimentally measured intensity of the guided waves confirms this prediction. Therefore, the triangular lattice with the parallel orientation can be seen as a higher-order generalization of the diamond lattice. Furthermore, comparing far field images of the lattice and guided waves allow us to conclude that the actual refractive index pattern has the *reduced symmetry* with respect to the lattice. Indeed, instead of six side-beams forming the lattice wave, there is only four side-beams in the guided wave meaning that the induced potential is unable to trap two side beams (top and bottom), and the guided-mode symmetry is reduced.

In contrast, the triangular lattices oriented perpendicular to the crystal axis display more complex transition from low to high saturation regimes, see Fig. 5(middle). Now we find that the "dipoles" are oriented parallel to the *c*-axis, and the guided wave has an essentially two-dimensional modulation. Even in the high-saturation regime when the refractive index profile resembles vertical stripes [cf. the square pattern in Fig. 1], the guided wave still has a visible modulation in the vertical direction. This is in contrast to the square pattern shown in Fig. 4 where the guided wave modulation also has the reduced symmetry.

Summarizing our theoretical and experimental results for different patterns with the edge-type phase dislocations induced in anisotropic photorefractive crystals, we would like to stress that the combined effect of anisotropy, saturation, and nonlocality can reduce significantly the symmetry of the optically-induced refractive index patterns. That is the case for the square and triangular lattices oriented parallel to the crystal axis. Nevertheless, as is found for the diamond and perpendicular triangular lattices, essentially two-dimensional modulation can be achieved, so that the isotropic saturable model can be employed to study this type of lattices.

5. Vortex lattices

Expanding the concept of the phase-modulated self-trapped nonlinear lattices, we follow the recent theoretical work [21] and introduce the so-called *vortex lattices*. Theoretically, these nonlinear waves bifurcate from the corresponding linear modes, that can be easily found from the linear paraxial equation 1 without nonlinear term, i.e. $n(I) = 0$. A linear superposition of two azimuthal modes $\sin\varphi$ and $\cos\varphi$ with azimuthal coordinate φ is known to give rise to a vortex beam with a phase dislocation, $\sim x + iy = r\exp(i\varphi)$. Similarly, superimposing two linear modes $U_{\rm lin}$ from Eq. (5), we obtain a vortex lattice of a square geometry,

$$U_{\rm vs}(x,y) = A(\sin x \sin y + i\cos x \cos y). \tag{7}$$

Numerical procedure to find the families of stationary nonlinear periodic waves with the vortex structure is similar to that described above. In Fig. 6 we present two examples of such lattices and compare low (a) and high (b) saturation regimes for the vortex lattice with a diamond-type intensity pattern. The parameters chosen are close to our experimental situation, in particular the relatively large periodicity of the lattice results in strong localization of separate lattice sites for large intensity, see Fig. 6(b,left).

Experimentally, we generate a square-type vortex lattice oriented diagonally to the principal axis of the crystal with a period of $57\,\mu$m. Applying an external DC electric field ($\mathscr{E} = 1300\,$V/cm) across the crystal provides the conditions for the formation of spatial solitons of $\sim 15\,\mu$m size and also influences the propagation of the periodic modes. Even at this high voltage and nonlinearity strength the output of the lattice does not deviate significantly from the shape of a linear wave [see Fig. 6(c, left)] and the position of the vortices is generally preserved, as shown in Fig. 6(c, middle). This is due to the fact that the profile of the nonlinear periodic lattice is fairly close to the corresponding non-diffracting linear wave.

In order to verify that the lattice indeed propagates in a truly nonlinear fashion, we probe the induced changes to the crystal refractive index. To do this, we send a broad plane-wave trough the crystal, by switching-off the SLM, and observe the modulation of the plane-wave

#10164 - $15.00 USD Received 3 January 2006; revised 12 March 2006; accepted 23 March 2006

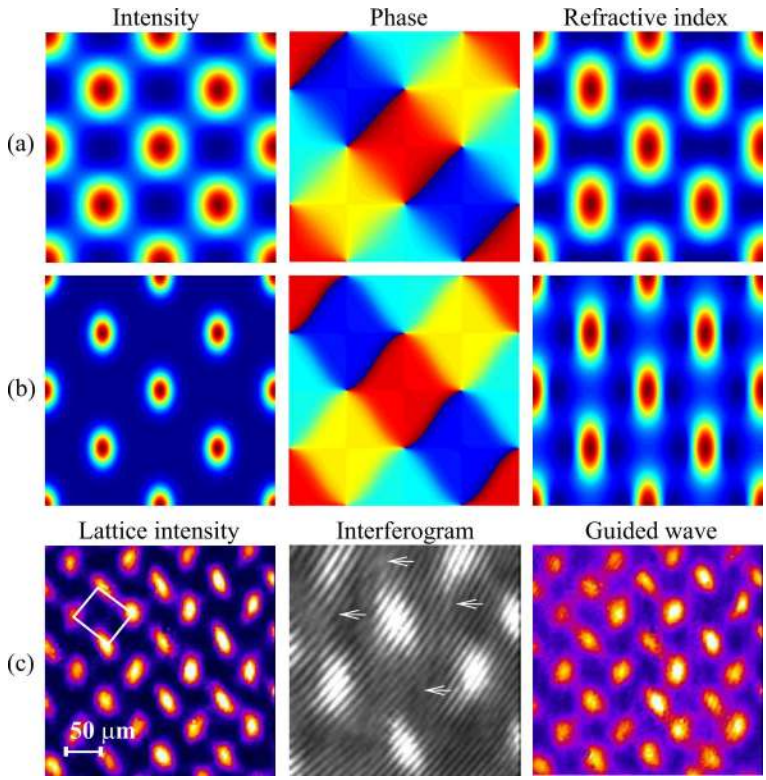

Fig. 6. Diagonally-oriented square vortex lattices in photorefractive self-focusing media. Numerically calculated stationary solutions are shown for $\Gamma = 11.8$ close to linear diffraction-free wave with $k = -0.1$ and $I_{\max} \simeq 0.42$ in (a), and in higher saturation regime with $k = 1.2$ and $I_{\max} \simeq 1.24$ in (b). (c) Experimentally observed vortex lattice with the period $57\,\mu$m: left - nonlinear output for bias 1.3 kV, middle - magnified top right part of the lattice interfering with a reference broad beam to monitor the position of the vortex dislocations (marked by arrows), right - intensity of the guided plane wave launched from the edge of the first Brillouin zone.

at the output. In the case of four-fold symmetry vortex lattice the generated plane wave is propagating exactly along the induced waveguides, e.g. in the middle of the first Brillouin zone. Output intensity distribution of the guided wave is shown in Fig. 6(c,right). As clearly seen, the plane wave is indeed modulated by the induced periodic potential, and we observe guiding of the probe beam at the maxima of the refractive index. This experimental observation is in a good agreement with the corresponding numerical simulations [see Fig. 6(a,b)].

The idea of generating vortex lattices as non-diffracting linear waves can be extended further to include more complex geometries such as hexagonal lattices shown in Fig. 7. Remarkably, despite the complex internal energy flows, these lattices can be seen as probably the simplest patterns with the three-fold symmetry created by the interference of only three plane waves [18] [cf. triangular patterns with six waves Eq. (7)],

$$U_{\rm vh}(x,y) = A\left[\exp(ix) + \exp\left(-ix/2 + i\sqrt{3}y/2\right) + \exp\left(-ix/2 - i\sqrt{3}y/2\right)\right]. \qquad (8)$$

In this type of patterns, the lattice sites create hexagonal closely packed lattice while the vortex-type dislocations form a honeycomb lattice with smaller spacing. Even though the vortices in

#10164 - $15.00 USD Received 3 January 2006; revised 12 March 2006; accepted 23 March 2006

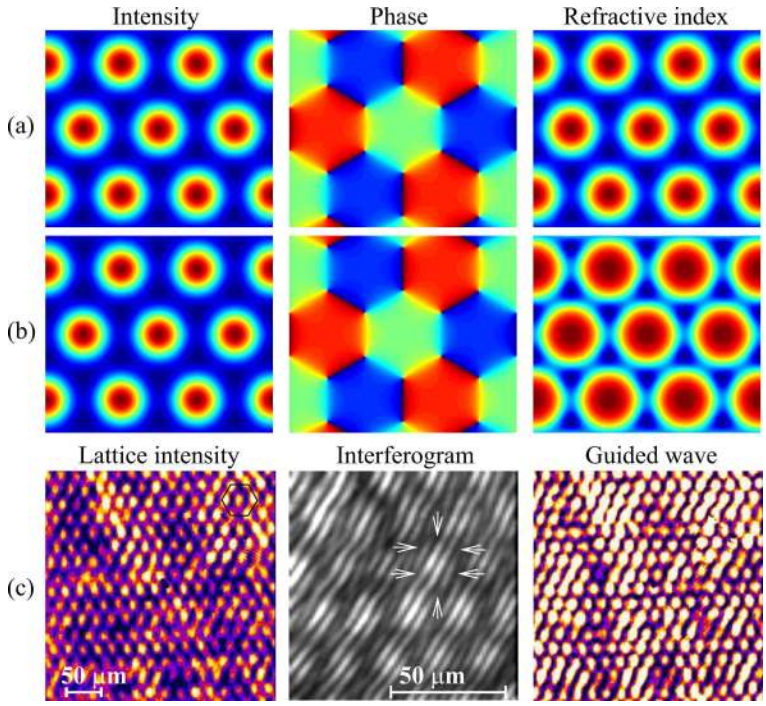

Fig. 7. Self-trapped hexagonal pattern with nested honeycomb vortex lattice, stationary solutions in isotropic saturable medium. The soliton constant $k = -0.8$ and peak intensity $I_{\max} \simeq 0.42$ in (a), and $k = -0.4$ and $I_{\max} \simeq 3.58$ in high saturation regime in (b). (c) Experimentally observed hexagonal vortex lattice of a period 22μm: left - nonlinear output for bias 1.3kV, middle - magnified bottom right part of the lattice interfering with a reference beam to identify the position of the vortices (marked by arrows), right - plane wave launched at the edge of the Brillouin zone and modulated by the induced index lattice.

the lattice are very closely packed, we demonstrate that such lattices can be experimentally generated and observed for rather small lattice periods, as shown in Fig. 7(c, left) for the period of $22\,\mu$m. The positions of the vortices in the lattice are also well preserved, as seen by the interferogramm in Fig. 7(c, middle). In order to probe the refractive index modulation in experiment, we send a plane wave trough the photorefractive crystal. By fast reprogramming of the modulator, we sent a plane wave propagating at the edge of the Brillouin zone, thus probing the bang-gap structure of the induced periodic refractive index modulation. In this way, we test not only the periodic modulations but also the inhomogeneities of the periodic pattern, since the gap in the transmission spectrum depends strongly on the structural defects and disorder. In our experiments, we observe a strong periodic modulation of the output wave with the maxima of the pattern located in between the lattice sites. This indicates an efficient excitation of the Bloch waves corresponding to the second band of the transmission spectrum. In addition, this observation proves that the induced nonlinear vortex lattice is homogeneous and stable.

Our theoretical analysis reveals that the vortex lattices possess distinct phase profiles, namely, instead of a smooth phase twist around each dislocation point, as one would expect for isolated optical vortices [17], the phase in the lattice experiences sharp jumps, and these phase steps can be identified as "soft" edge dislocations (with phase difference less than π). The number of such steps depends on the symmetry of the lattice [see Fig. 6 and Fig. 7], so that each lattice site has a fairly well defined phase, as shown by different colors. Indeed, the phase steps for

#10164 - $15.00 USD Received 3 January 2006; revised 12 March 2006; accepted 23 March 2006

the square vortex lattice are equal $2\pi/4 = \pi/2$, thus there are four colors in the phase profiles of Fig. 6, dark blue (0), light blue ($\pi/2$), yellow (π), and red ($3\pi/2$). In contrast, the phase step for the hexagonal lattice is $2\pi/3$ (each vortex is "built" with three lattice sites), so there is almost no yellow. This phase behavior resembles the structure of soliton clusters [27] with different azimuthal numbers [28], as well as the structure of discrete vortex solitons in periodic lattices [29, 30]. Furthermore, as we discussed earlier in Ref. [21], the intensity profiles of the vortex lattices do not differ significantly in the cases of a linear medium, and self-focusing or self-defocusing nonlinear media, in contrast to the bright and dark vortex solitons. Therefore, the vortex lattices presented above provide a link between the singular beams in linear and nonlinear bulk media, as well as discrete vortices in external periodic potentials [17].

6. Conclusions

We have studied theoretically and generated experimentally, in a biased photorefractive crystal, two-dimensional nonlinear photonic lattices of several different symmetries. Employing a nonlocal anisotropic nonlinear model, we have described the structure and properties of the self-trapped spatially-periodic nonlinear photonic lattices with out-of-phase neighboring sites, as well as chessboard-like and triangular nonlinear patterns. For the triangular lattices, we have found two distinct classes of optically-induced refractive index patterns with one of the edge dislocation lines oriented parallel or perpendicular to the *c*-axis of the crystal. We have demonstrated that the highly anisotropic periodic refractive index induced by the lattices differs significantly from its isotropic counterpart, and it depends strongly on the lattice orientation. We have expanded our theoretical approach to the periodic lattices with nested arrays of vortex-type phase dislocations, or vortex lattices, and have generated experimentally vortex lattices with two different symmetries. The square vortex lattice acquires a diamond-like intensity pattern, while for the six-fold symmetry we have demonstrated that a hexagonal intensity pattern can be generated with the vortices arranged in a honeycomb lattice.

Acknowledgments

This work was produced with the assistance of the Deutsche Forschungsgemeinschaft in the framework of the graduate school "Nonlinear Continuous Systems". We thank the Alexander von Humboldt Foundation, the Australia-Germany Exchange Program of the Australian Academy of Science, and the Australian Research Council. DT acknowledges support by the Konrad-Adenauer-Stiftung e.V. We thank Andrey Sukhorukov for critical reading of this manuscript and useful comments. Anton Desyatnikov acknowledges Sergei Odoulov for enlightening discussions of the triangular patterns.

#10164 - $15.00 USD Received 3 January 2006; revised 12 March 2006; accepted 23 March 2006